nature communications

Article

https://doi.org/10.1038/s41467-025-58567-y

The integrin repertoire drives YAP-dependent epithelial:stromal interactions during injury of the kidney glomerulus

Received: 15 November 2023

Accepted: 27 March 2025

Published online: 08 April 2025

Check for updates

Evelyne Huynh-Cong[1,2,9], Victoria Driscoll[3], Sandrine Ettou[1,2], Keith Keller[4,5], Amha Atakilit[6], Mary E. Taglienti[1], Saurabh Kumar[1,10], Astrid Weins[4], Valerie A. Schumacher[1,2,3,7,11] & Jordan A. Kreidberg[1,2,3,7,8,11]

The kidney glomerulus is a filtration barrier in which capillary loop architecture depends on epithelial-stromal interactions between podocytes and mesangial cells. Podocytes are terminally differentiated cells within the glomerulus that express YAP and TAZ. Here we test the hypotheses that YAP and TAZ are required in podocytes to maintain capillary loop architecture and that shifts in the integrin repertoire during podocyte injury affect transcriptional activity of YAP and TAZ. Loss of YAP in podocytes of adult mice renders them more sensitive to injury, whereas loss of both YAP and TAZ in podocytes rapidly compromises the filtration barrier. α3β1 and αvβ5 are two prominent integrins on murine podocytes. Podocyte injury or loss of α3β1 leads to increased abundance of αvβ5 and nuclear localization of YAP. In vitro, blockade of αvβ5 decreases nuclear YAP. Increased αv integrins are found in human kidney disease. Thus, our studies demonstrate the crucial regulatory interplay between cell adhesion and transcriptional regulation as an important determinant of human disease.

Epithelial-stromal interactions play a critical role in human disease. In many instances, an underlying stroma produces soluble growth factors or an extracellular matrix (ECM), both of which may have profound effects on epithelial behavior within a cellular microenvironment[1–3]. Conversely, the stroma may respond to biomechanical changes in the epithelium[4]. These interactions have primarily been studied in relation to tumor progression. Here we examine a unique and essential non-neoplastic microenvironment crucial to maintaining normal kidney function in the glomerulus, that is between the podocyte and the mesangial cell[5]. These two cell types maintain the capillary loop architecture within the glomerulus that is necessary to establish the glomerular filtration barrier (GFB), thereby allowing proper filtration of water and electrolytes, while retaining proteins such as albumin and immunoglobulins in the circulation. Breakdown of the GFB, that occurs in conditions such as focal segmental glomerulosclerosis (FSGS) or diabetic nephropathy, results in massive loss of albumin from the circulation[6], and often requires dialysis or kidney transplant for survival, accounting for a major component of national health expenditures[7].

Many studies over the past two decades have revealed podocyte injury to be the incipient event leading to breakdown of the GFB and the onset of chronic kidney disease[6]. Relatively less attention has been

[1]Department of Urology, Boston Children's Hospital, Boston, MA, USA. [2]Department of Surgery, Harvard Medical School, Boston, MA, USA. [3]Division of Nephrology, Beth Israel Deaconess Medical Center, Boston, MA, USA. [4]Department of Pathology, Brigham and Women's Hospital and Harvard Medical School, Boston, MA, USA. [5]Broad Institute of Harvard and MIT, Cambridge, MA, USA. [6]Lung Biology Center, Department of Medicine, University of California San Francisco, San Francisco, CA, USA. [7]Department of Medicine, Harvard Medical School, Boston, MA, USA. [8]Harvard Stem Cell Institute, Cambridge, MA, USA. [9]Present address: for EHC: Evotec, Gottinggen, Germany. [10]Present address: for SK: University of Massachusetts Chan Medical School, Worcester, MA 01605, USA. [11]Present address: for VAS and JAK: Division of Nephrology, Beth Israel Deaconess Medical Center, Boston, MA 02215, USA.
e-mail: VSchumac@bidmc.harvard.edu; Jkreidbe@bidmc.harvard.edu

paid to the critical interactions between podocytes and mesangial cells that maintain the capillary loop architecture of the glomerulus[5]. Podocytes and mesangial cells interface through two components of the ECM, the glomerular basement membrane (GBM) and the mesangial matrix. As such, the integrin receptors for the ECM on podocytes and mesangial cells play an important role in establishing and maintaining the GFB[8,9].

YAP (Yes1 associated transcriptional regulator) and TAZ (Transcriptional coactivator with PDZ-binding motif, also known as WW domain-containing transcription regulator protein 1, WWTR1) are highly related transcriptional effectors of the HIPPO signal transduction pathway (and other pathways) that associate with TEAD transcription factors to regulate target gene expression[10]. The nuclear localization of YAP and TAZ, and thus their transcriptional activity, may be determined by integrin-mediated mechanosensation of the adjacent ECM[10]. We have recently demonstrated that podocytes respond to injury by reprogramming their transcriptome, initially increasing the expression of components of the GFB[11].

Podocytes are highly specialized cells found in the kidney glomerulus (Fig. 1A). Their cell body projects major extensions known as primary processes, that extend into smaller foot processes (FP) (Fig. 1B). Foot processes (FP) are anchored to the glomerular basement membrane (GBM) and interdigitate with the FP from adjacent podocytes, forming a tight scaffold encircling the glomerular capillaries. Podocyte FPs, the GBM, and the endothelium of glomerular capillaries constitute the 3 layers of the glomerular filtration barrier (GFB) that prevents leakage of plasma proteins such as albumin from the circulation. In between FPs, there exists a specialized cell-cell junction known as the slit diaphragm, composed of proteins such as nephrin and podocin, that confer permselective properties to the GFB. Podocyte injury and loss is the incipient event leading to highly debilitating forms of chronic kidney disease, including focal segmental glomerular sclerosis (FSGS), a human condition which eventually leads to glomerular scarring following podocyte loss. However, podocyte FPs are dynamic and under reversible conditions such as minimal change disease, they are able to retract and then later re-establish their interdigitations to restore the GFB.

In this study we demonstrate that YAP and TAZ have a major role in podocytes, required for expression of genes vital to podocyte function. The nuclear translocation of YAP and TAZ in podocytes is dependent on the integrin repertoire and increases in response to injury. These changes in YAP localization and integrin expression are also observed in humans with glomerular disease. Moreover, the epithelial-stromal interactions responsible for maintaining glomerular architecture are disrupted in the absence of YAP and TAZ, as manifested by loss of the GFB and disorganized localization of podocytes and mesangial cells. Podocytes are terminally differentiated cells. Therefore, this study demonstrates that the integrin repertoire and the resultant nuclear localization of YAP/TAZ in terminally differentiated cells may undergo significant changes in response to injury.

Results

Podocyte expression of YAP and TAZ is required to maintain glomerular structure and function

Our previously published study demonstrated a primary role for the Wilms' tumor-1 (WT1) transcriptional factor in directing transcriptional reprogramming in response to podocyte injury[11]. We found predicted TEAD binding sites commonly adjacent to those bound by the WT1 transcription factor (TF). These WT1 and putative TEAD/YAP/TAZ target genes included genes important in maintaining the GFB, such as *Nphs1, Nphs2*, *Synpo*, and many others. Previous studies of YAP and TAZ in podocytes used constitutive tissue-specific knockouts or inducible gene inactivation that was not restricted to podocytes[12–14]. In this study, we used inducible gene inactivation in adult mice to generate inducible podocyte-specific knockouts of *Yap* and *Wwtr1* (the gene that encodes TAZ). Single inactivation of *Yap* or *Wwtr1* in 8-week adult mice did not result in histological changes or proteinuria by 10 weeks post gene inactivation (Fig.1C and Fig. S1A, quantification in Table S1), indicating YAP or TAZ are unlikely to have required non-redundant functions in podocytes of adult mice under non-injury conditions. Therefore, we generated an inducible podocyte-specific double knockout of *Yap* and *Wwtr1* in adult mice: *Nphs2-iCre; Yap*$^{fl/fl}$; *Wwtr1*$^{fl/fl}$, (henceforth referred to as DKO mice). Periodic acid–Schiff (PAS) staining of kidney sections from homozygous double knockout mice showed the collapse of glomerular capillaries with obstruction of capillary lumina and reactive parietal epithelium (Fig. 1C, time course of DKO shown in Fig. S1A, Histological analysis in Table S1). Protein casts in the tubules provided additional evidence for a breakdown of the GFB (Fig. 1C, Fig. S1B, and Table S1). On the other hand, little interstitial fibrosis was apparent. DKO mice had pale-appearing kidneys (Fig. 1D), and rarely survived beyond 14 days post-induction. Loss of both YAP and TAZ resulted in the onset of massive proteinuria within 8 days (Fig. 1E), demonstrating that there is indeed a crucial role for YAP/TAZ function in terminally differentiated cells such as podocytes. Electron microscopic analysis of DKO mice revealed dilated capillaries by 5 days post-induction, that had considerably worsened by day 8 (Fig. 1F and S1C). Immunofluorescent co-staining for YAP/TAZ and WT1 confirmed loss of YAP and TAZ (Fig. S2A, B). Foot process effacement was also present (Fig. 1F, G). Furthermore, we were able to demonstrate a gene-dosage phenotype using *Nphs2-iCre;Yap*$^{fl/fl}$;*Wwtr1*$^{fl/+}$, or *Nphs2-iCre;Yap*$^{fl/+}$ *Wwtr1*$^{fl/fl}$; each of which developed proteinuria within 14 days post-induction (Fig. 1E, lower magnification images of all genotypes at 8 days post-induction shown in Fig. S1B).

Quantitative analysis of mRNA levels in glomeruli of DKO mice found greatly reduced levels of *Nphs1*, *Nphs2*, and *Synpo*, encoding nephrin, podocin, and synaptopodin, respectively (Fig. 2A). This was not due to loss of podocytes, whose numbers remained similar through day 8 post-induction (Fig. S2C). Immunofluorescent staining confirmed greatly reduced levels of nephrin, much of which was not localized to capillary loops, consistent with the high level of proteinuria in DKO mice (Fig. 2B, C). Synaptopodin protein was relatively less reduced (Fig. 2B, C), but its localization was atypically more diffuse in the regions where nephrin was missing around the capillary loops (Fig. 2B). Protein levels of nephrin and synaptopodin were quantified by measurement of immunofluorescence intensity of individual glomeruli (Fig. 2C). Similarly to the electron micrographs in Fig. 1F and S1, co-visualization of nephrin and endomucin, a marker of endothelial cells (Fig. 2D) revealed dilated capillary loops in glomeruli of DKO mice. Our previous genome-wide analysis of potential transcription factor binding sites adjacent to those bound by WT1 found TEAD motifs to be the most common[11]. Predicted TEAD binding sites were present at 5 of 6 WT1 binding sites at *Nphs2* or *Synpo* (*Nphs2-2* is the exception) (Fig. 2E). ChIP-qPCR for YAP confirmed binding, that was absent in DKO mice (Fig. 2F). These observations suggest that YAP/TAZ/TEAD, along with WT1, constitutes a core set of TFs required to maintain expression of genes encoding components of the GFB and podocyte cytoskeleton.

YAP translocates into the podocyte nucleus after injury

The observation that YAP/TAZ are essential for the proper function of a terminally differentiated cell such as the podocyte raised the question of whether YAP/TAZ also has a role in the response to injury. This is especially important in terminally differentiated cells that are incapable of proliferating to replace lost cells. The BALB/c inbred strain of mice is particularly sensitive to adriamycin (ADR)-induced podocyte injury and loss, making it the prototypic strain to model podocyte injury leading to FSGS[15]. Under physiological conditions, YAP is found in both the cytoplasm, partially overlapping with nephrin, and in the nucleus (Fig. 3A, B). Treatment of BALB/c mice resulted in a significantly increased amount of YAP in the nuclei of podocytes

https://doi.org/10.1038/s41467-025-58567-y

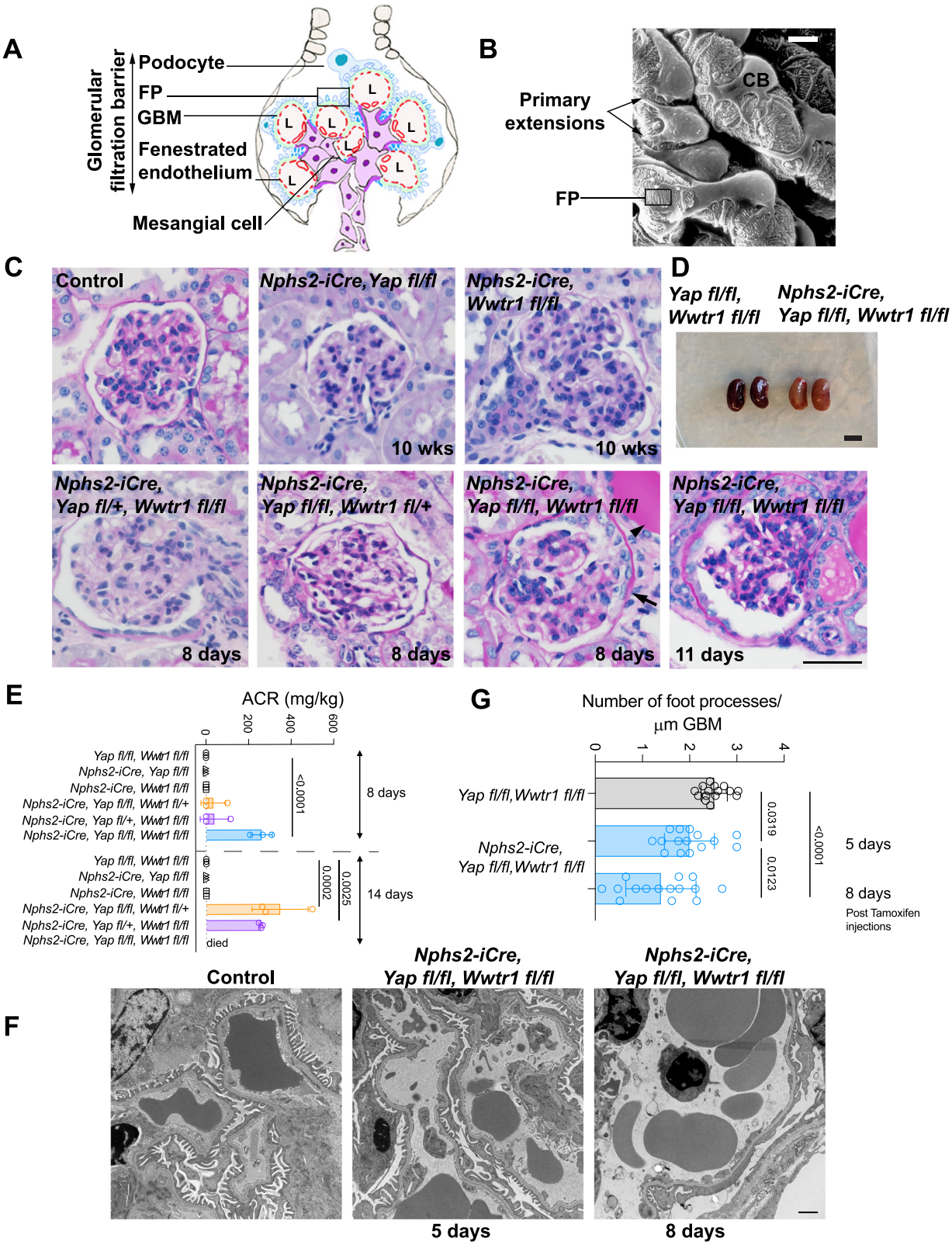

quantified by co-localization with the podocyte nuclear marker p57 (Fig. 3B, C). A limitation of the Balb/c ADR model is that there is limited recovery of proteinuria[15]. Using a second model of glomerular injury that allows recovery of foot process architecture[16–18], increased nuclear localization of YAP was again observed after treatment of outbred mice with nephrotoxic serum (NTS) compared with normal sheep serum (NSS) (Fig. S3). NTS is partially directed against β1 integrins, suggesting that compromising podocyte adhesion to the GBM may provoke nuclear localization of YAP[19]. In contrast to the Adriamycin model, proteinuria eventually resolves in NTS-treated mice, and nuclear localization of YAP returns to baseline (Fig. S3). These observations suggest that podocyte injury results in translocation of YAP to the podocyte nucleus, and that this translocation may be a major component of the podocyte response to injury.

Fig. 1 | Loss of the glomerular filtration barrier after podocyte-specific loss of YAP and TAZ in adult mice. A Schematic diagram of podocyte structure. Note that mesangial cells (purple) provide a support structure for capillary loops (L). **B** Example of scanning electron micrograph of glomerular capillary loops. Primary extensions and foot processes (FP) (provided by W. Kriz, Heidelberg, Germany). Size bar = 10 µm. **C** PAS stained representative glomeruli of *Yap* and *Wwtr1* mutant mice, genotypes at the top of each panel. At least $N = 3$ for all genotypes. The time post tamoxifen induction is shown in each panel. Arrow: parietal expansion; arrowhead: protein cast. Size bar = 20 µm. **D** Photograph showing pale-appearing mutant kidneys. Size bar = 5 mm. **E** Urine albumin:creatinine ratios of control and mutant mice, plotted as mean values ± SD. Time points on the right. For each time point, one-way analysis of variance (ANOVA) with Tukey's multiple comparisons test was used, p values in figure. $n = 3$ replicates. **F** Electron micrographs (10,000X) showing foot process effacement and capillary dilation in DKO mice at 5 and 8 days post-induction. Size bar 1 µm. **G** Quantification of foot process effacement. D0 $n = 2$; d5 $n = 1$; d8 $n = 1$ mice; each dot represents one glomerulus analysed. One-way ANOVA and Tukey's multiple comparison used to measure significance. d0 vs. d5, p values in figure.

To determine whether the gene-dosage phenotype for *Yap* became more pronounced during the response to injury, we treated *Nphs2-iCre*; *Yap*$^{fl/fl}$ mice with Adriamycin (Fig. 3D). At the dose of ADR used in this experiment, treatment of control *Yap fl/fl* mice does not lead to detectable proteinuria (Fig. 3E). However, the absence of YAP in podocytes leads to high levels of albumin present in urine by 8 weeks (Fig. 3E), though this did not result in changes detectable by PAS staining (Fig. S4, Quantification in Table S2).

YAP is required for the repair of the podocyte cytoskeleton

Podocytes have a complex morphology that is highly dependent on their cytoskeletal organization and specialized patterns of adhesion to their underlying ECM. The greater sensitivity of YAP-deficient podocytes to ADR-induced injury in vivo led us to hypothesize that YAP plays an important role in podocyte cytoskeletal organization. It has been possible to model aspects of podocyte cytoskeletal organization using immortalized murine podocyte cell lines that are allowed to differentiate in vitro. Therefore, to further characterize the role of YAP during podocyte repair at the cellular level, we used two independent siRNAs to obtain YAP-deficient differentiated podocytes (Fig. 4A and Fig. S5A). Loss of YAP in cells that were initially fully spread causes them to retract (Fig. S5B). The size of individual focal adhesions, as measured by staining for paxillin (Fig. S5C), did not change, but the number of focal adhesions per cell were significantly decreased (Fig. S5D), such that the total focal adhesion area per cell area was also decreased (Fig. S5E). In addition, actin stress fibers were diminished across the cell body (Fig. S5F). A role for YAP in dynamic cytoskeletal organization, that is crucial in response to injury, was modeled by trypsinizing siRNA-treated cells and allowing them to re-adhere and spread (Fig. 4B). Again, stress fibers in *Yap* siRNA-treated cells were decreased across the cell body and upon re-adhering, cells spread poorly compared to scrambled siRNA-treated cells (Fig. 4C, D). Actin polymerization into stress fibers is mediated by RhoGTPase. Thus, decreased activity of RhoGTPase might be responsible for the cytoskeletal defects in si*Yap*-treated cells. In particular, RhoA has been shown to be crucial in recruiting and activating downstream effectors of actin polymerization and the assembly of the contractile apparatus, such as formins, cofilin, and myosin light chain kinase[20]. Indeed, both phospho-cofilin and phospho-myosin light chain-2 (pMLC2) were decreased in *Yap* siRNA-treated cells and failed to increase as cells spread after being plated (Fig. 4A). The formation of a myosin-rich ring that confers contractile properties to the cortical actin cytoskeleton is an important step in cellular morphogenetic processes that ultimately project extensions from the cell body[21]. Such a process is hypothesized to be fundamental to podocytes reestablishing projections during the recovery from injury. The majority of scrambled siRNA-treated cells assembled a contractile ring during the process of spreading, as visualized by staining for pMLC2 and qualitatively scoring cells at 4 and 24 hr post trypsinization based on localization of pMLC2 (Fig. 4E–G). In contrast, the great majority of *Yap* siRNA-treated cells failed to form contractile rings and spread poorly after re-adhering.

The dependency on YAP for assembly of the contractile apparatus in vitro led us to determine whether there is a similar dependency in podocytes in vivo during the response to injury. In control podocytes in vivo, there is little pMLC2 present, indicating that the contractile apparatus is not highly active. After ADR treatment, pMLC2 is highly abundant in both primary extensions (co-stained with nestin) and foot processes (co-stained with nephrin) (Fig. 4H, reproduced for clarity with magnified insets in Fig. S6). This observation, consistent with previously published studies, indicates that the contractile apparatus becomes highly activated when primary extensions and FP are re-established after injury. Similarly to the in vitro observations, after injury, there were much lower levels of pMLC2 in podocytes of *Yap* mutant mice (Fig. 4H and Fig. S6). Thus, loss of YAP in podocytes impairs the plasticity of their cytoskeletal architecture in response to injury.

Yap-dependent epithelial-stromal architecture and repair

The convolutions of glomerular capillary loops are anchored by adhesive interactions where mesangial cells and the ECM they produce (referred to as the mesangial matrix) are juxtaposed to endothelial cells (schematized in Fig. 1A). Capillary loops are also otherwise supported by the scaffold formed by interdigitating podocyte foot processes, that in turn adhere to the GBM. While podocytes predominantly adhere to capillaries, there are also areas between two adjacent capillary loops where podocytes are directly juxtaposed to mesangial cells and their matrix. The area where the podocyte interfaces with the mesangial cells has been referred to as the "mesangial pedestal"[22]. The factors governing epithelial:stromal interactions between podocytes and mesangial cells during the response to injury remain incompletely understood, but are crucial to maintaining the integrity of the GFB[5]. Our observations described thus far demonstrate that podocyte expression of YAP/TAZ is required to maintain glomerular architecture, and that podocyte injury leads to increased nuclear localization of YAP. As the loss of both YAP and TAZ quickly leads to a complete loss of glomerular function, we used mice with induced podocyte-specific inactivation of *Yap* only to examine how YAP/TAZ are involved in establishing and maintaining the podocyte-mesangial relationship, and in the response to injury. In normal glomeruli, groups of mesangial cells, identified through the expression of the intermediate filament protein desmin, form a nexus that mechanically supports adjacent capillary loops in place. (Figs. 1A, 5Aa). In *Yap* mutant mice, capillaries are deformed (Fig. 5Ab, quantification of circularity for Fig. 5a–d in Fig. 5B). The co-localizations of activated β1 integrin with desmin or α3β1 integrin reveal dysmorphic grouping of mesangial cells, increased amounts of desmin, (Quantification of desmin staining in Fig. 5C) and distortion of capillary loop architecture (Fig. 5Aa vs. Ab, 5Da vs. Db, schematized in Fig. 5E. Distortion of the desmin localization is also shown by co-localization of nephrin and desmin (Fig. S7). This is further supported by electron microscopic images showing elongated-appearing capillary loops in *Yap* mutant mice 8 weeks after gene inactivation (Fig. S8) and by co-staining for nephrin and the endothelial marker endomucin (Fig. S9). Activated-β1 integrin, used to demonstrate high-affinity interactions of integrins with the ECM, appears more abundant in *Yap* mutant mice (Fig. 5Aa vs. b), and is present both on mesangial cells that co-stain for desmin (Fig. 5Aa vs. Ab) and on podocytes that co-stain for α3β1

https://doi.org/10.1038/s41467-025-58567-y

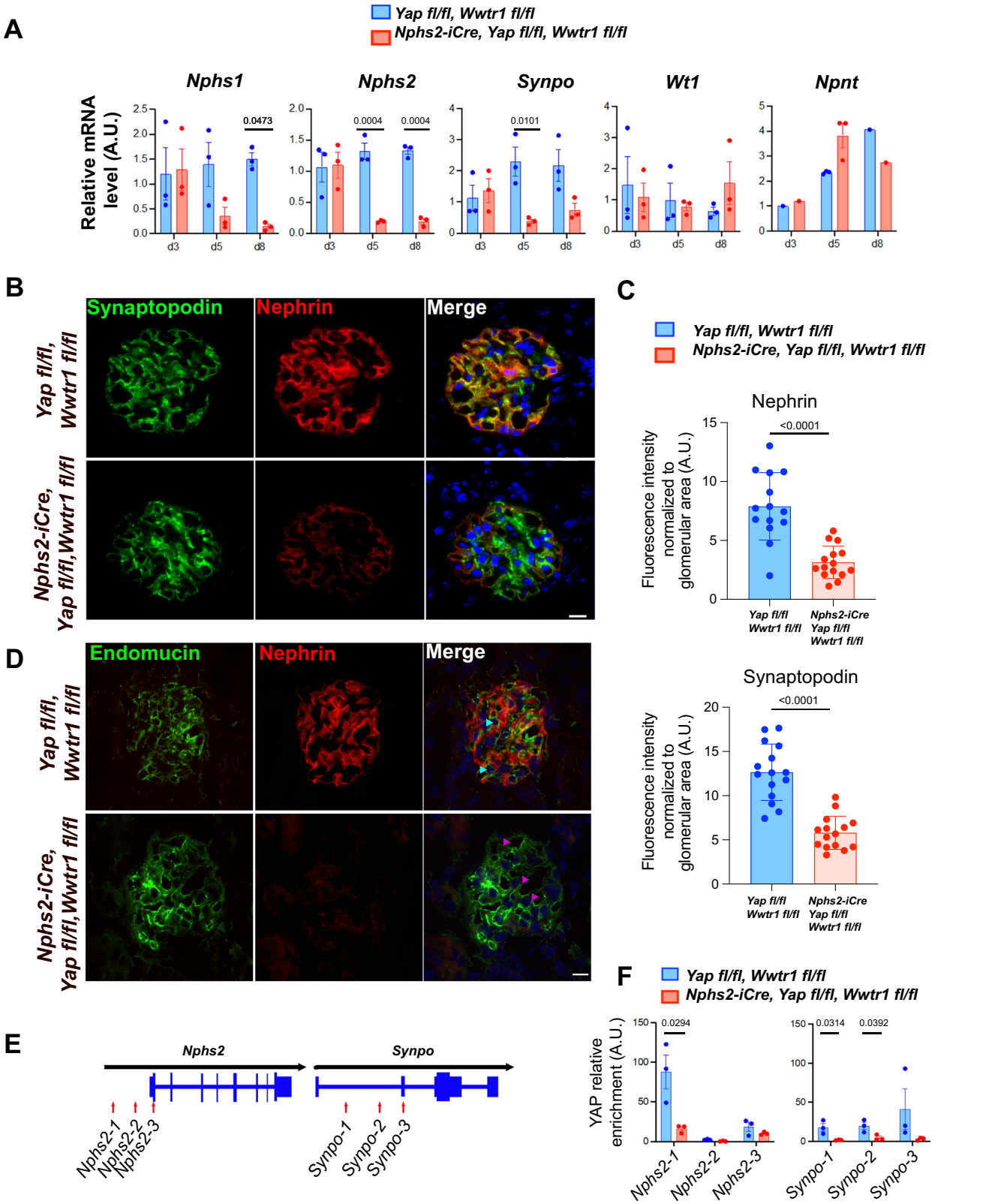

Fig. 2 | YAP/TAZ are required to maintain podocyte gene expression. A RT-qPCR of mRNA levels in DKO mice, plotted as mean values ± SEM. Levels are normalized to 1.0 for control D3. Time points at the bottom. Two-way ANOVA with Sidak's multiple comparisons test was used, *p* values in figure. ($n = 3$ mice per group, except for *Npnt* d3 and 8, $n = 1$). **B** Synaptopodin and nephrin co-localization. Top row, control, bottom row DKO, at D8 post-induction with tamoxifen. **C** Quantification of immunofluorescence in (**B**), plotted as mean ± SD, $n = 3$ mice, five glomeruli from each mouse; each dot represents one glomerulus; Statistical analysis: two-tailed unpaired *t*-test, *p* values in figure. **D** Endomucin co-stained with nephrin. Blue arrowheads mark normal size capillaries in control, pink arrows mark dilated irregularly shaped capillaries in DKO. **E** Schematic showing the location of WT1 binding sites used for ChIP-qPCR at *Nphs2* and *Synpo*. **F** YAP ChIP-qPCR at the sites shown in (**E**) two-tailed unpaired *t*-test used to compare data, *p* values in figure. Size bar for (**B**, **D**) = 10 µm. ($n = 3$ per group).

https://doi.org/10.1038/s41467-025-58567-y

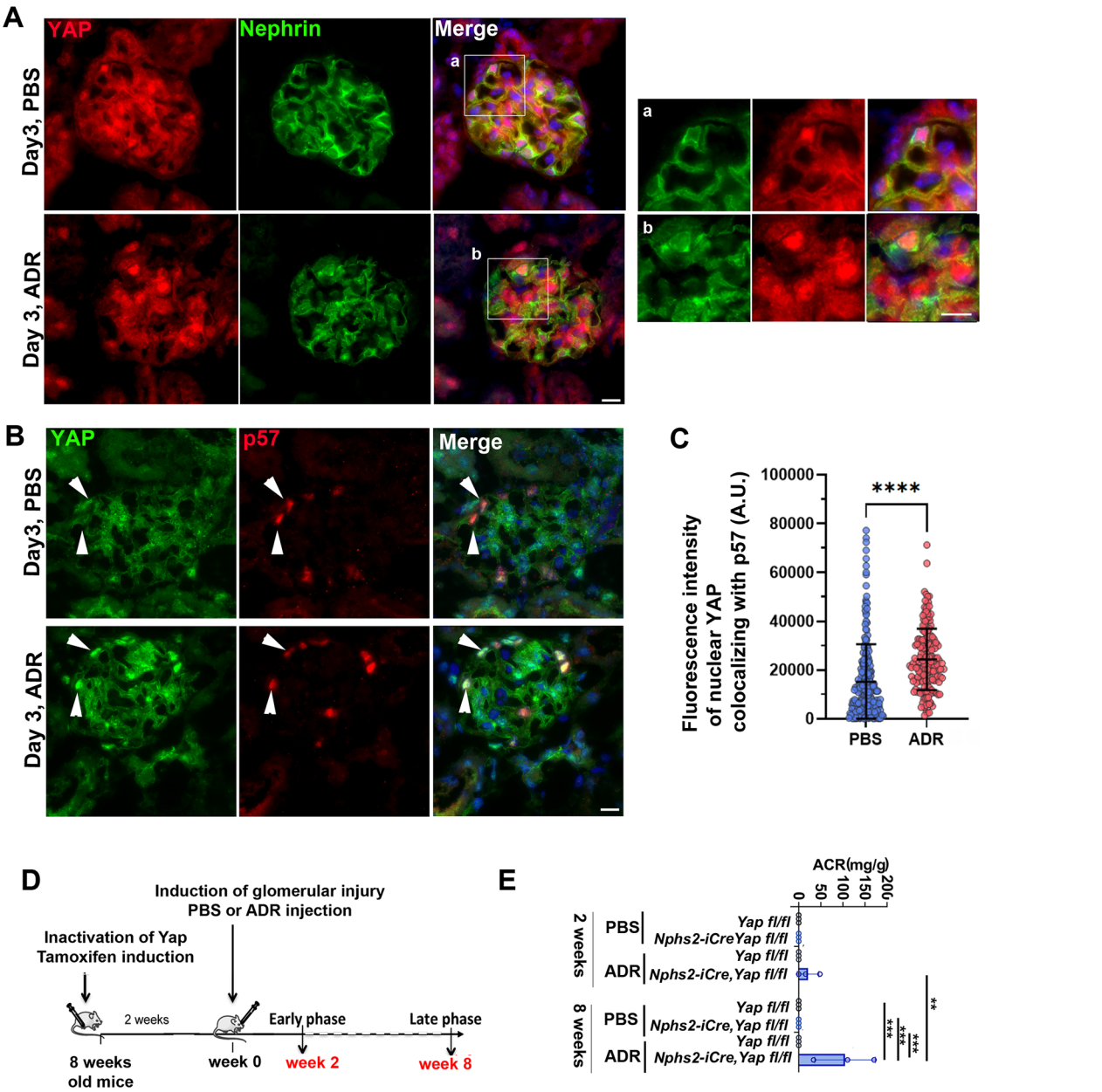

Fig. 3 | YAP translocation into the nucleus after injury and increased sensitivity to podocyte injury in *Yap* mutant mice. A Co-localization of YAP and nephrin, top row: control, bottom row 3 days post ADR in BALB/c mice, representative of three independent experiments. Insets show magnified images boxed in merge panels. Size bar = 10 µm. **B** Co-localization of YAP and p57, top row: control, bottom row 3 days post ADR in BALB/c mice. Size bar = 10 µm. **C** Quantification of nuclear localization of YAP in cells co-expressing podocyte marker p57 in BALB/c mice. Mann–Whitney two-tailed test: $^{****}P < 0.0001$. $n = 3$ per group. **D** Scheme of time points urine/tissue collection for ADR injection into *Nphs2-CreERtT2, Yap fl/fl* mice and **E** Urine albumin:creatinine ratios of control and mutant mice in (**D**), plotted as mean values ± SD, two-way ANOVA with Sidak's's multiple comparison test, 2wk *Cre* + ADR vs 8wk *Cre* + ADR $^{***}p = 0.0097$, 8wk *Cre*-ADR vs 8wk Cre+ADR $^{***}p = 0.0005$, 8wk *Cre* + PBS vs 8wk *Cre* + ADR $^{***}p = 0.0005$, 8wk *Cre*-PBS vs 8wk *Cre* + ADR $^{***}p = 0.0005$. $n = 3$ per group.

integrin (Fig. 5Da vs. Db). Indeed, most of the increase in activated β1 integrin appears to be on mesangial cells (Fig. 5Aa vs. Ab), suggesting a mechanosensory response in those cells to the distorted architecture caused by loss of YAP in podocytes. Furthermore, desmin localization extends further around the capillary perimeter, suggesting that mesangial cells are adjacent to a greater portion of the capillary circumference (Fig. 5Aa vs. Ab). Recent studies have identified α8β1 integrin on mesangial cells and its ligand, nephronectin, as a component of the glomerular basement membrane where podocytes are juxtaposed to mesangial cells[22]. However, we did not find reduced *nephronectin* mRNA in DKO glomeruli (Fig. 2A), suggesting a more complex etiology for this phenotype. In glomeruli, localization of α3β1 integrin partially overlaps with active β1 (Fig. 5D), suggesting that the non-overlapping staining, where only activated β1 is present, represents α8β1 or other β1 integrins on mesangial cells. In ADR-treated *Yap* mutant mice, there is not only a more dramatic loss of normal architecture, demonstrated by dilated capillary loops and more disorganized localization of desmin (Fig. 5Ab vs Ad and Fig. S7), but also a high level of proteinuria by 8 weeks post ADR treatment (Fig. 3E). Together these observations demonstrate that the absence of YAP renders podocytes far more sensitive to injury and impairs the stromal:epithelial interactions between podocytes, endothelial cells, and mesangial cells, that preserve the structure and function of the glomerulus.

https://doi.org/10.1038/s41467-025-58567-y

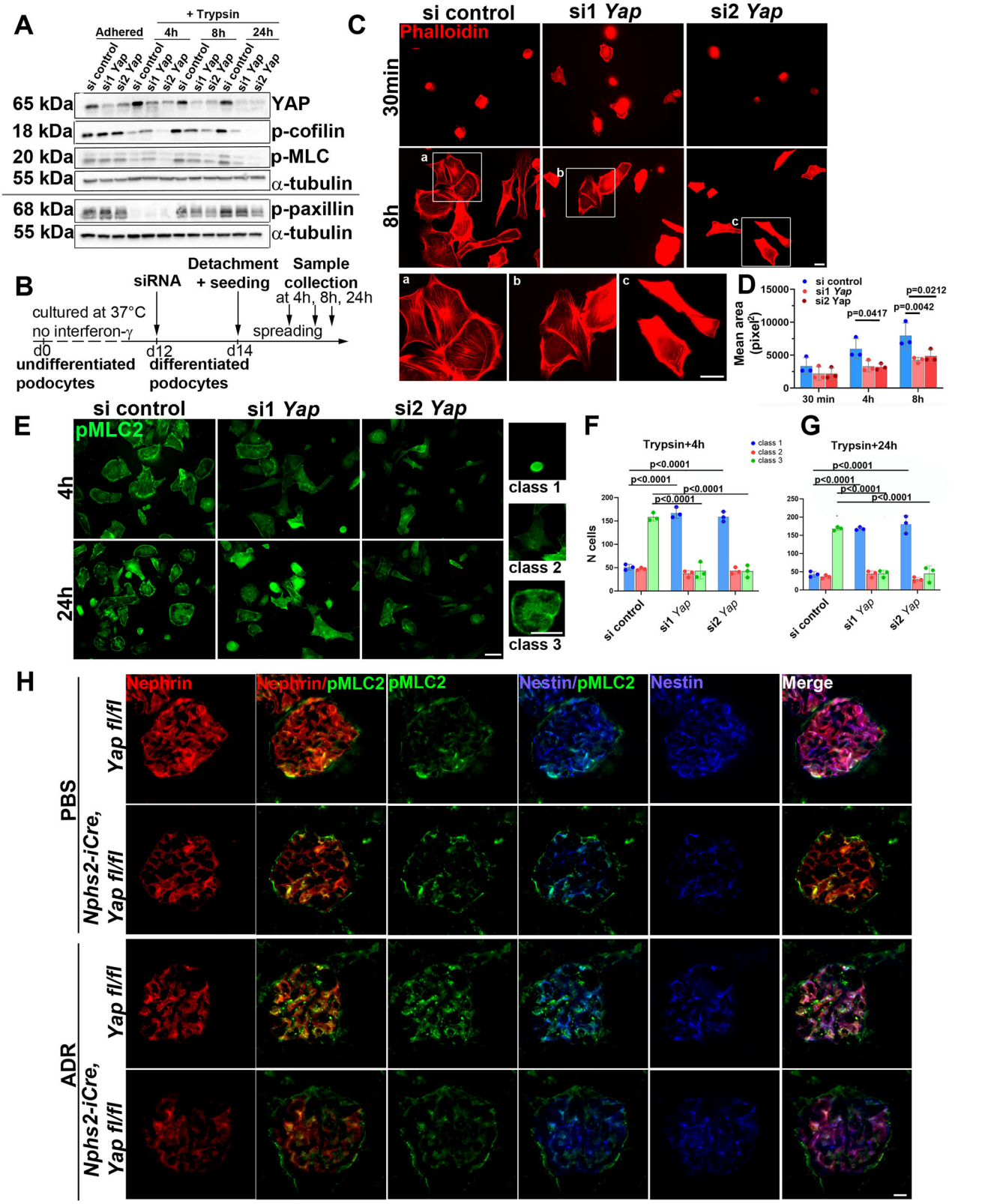

Alterations in integrin localization during glomerular injury

YAP/TAZ localization is known to be affected by integrin recognition of the extracellular matrix (ECM); generally, a "stiffer" ECM promotes nuclear localization while a more "relaxed/soft" ECM maintains YAP/TAZ in the cytoplasm[23–25]. We hypothesized that the adhesive mechanisms that govern glomerular architecture may determine the localization of YAP/TAZ in podocytes. Indeed, in the cortex of the normal kidney, activated β1 integrin appears to be far more abundant in glomeruli than in adjacent tubules (Fig. S10), serving to emphasize how active integrin-mediated mechanosensation is part of normal glomerular function. Moreover, changes in these adhesive interactions during glomerular injury may constitute the basis for the increased nuclear translocation of YAP. Therefore, using ADR-mediated injury in Balb/C mice, we investigated how integrin:ECM interactions changed

Fig. 4 | Deficient cytoskeletal reorganization in *Yap*-deficient podocytes in vitro and in vivo. A Western blots of proteins indicated at the right of each row. Cells were adhered, or time points re-adhered at trypsinization, as shown at the top. Each group of three lanes shows representative scrambled control and treated with siRNA1 or siRNA2 for *Yap*. Representative of three independent experiments. **B** Scheme of in vitro detachment and re-adhesion experiments. **C** Phalloidin stain of immortalized podocytes at time points after trypsinization and re-adhesion. Size bar = 20 µm. a–c show magnification of inserts. Size bar = 20 µm. **D** Quantification of cell areas at 30 min, 4 h, and 8 h after adhesion, plotted as mean values ± SD. Two-way ANOVA with Sidak's multiple comparisons test was used, *p* values in figure. $n = 3$ replicates. **E** pMLC2 localization after *Yap* siRNA, trypsinization, and re-adhesion. Sample class 1, 2, and 3 cells shown at right. Size bar = 50 µm. **F**, **G** Manual quantification of class appearance of control and *Yap* siRNA treated cells at 4 h (**F**) and 24 h (**G**) after trypsinization and re-adhesion plotted as mean values ± SD. Two-way ANOVA with Dunnett's multiple comparisons test was used, *p* values in figure. From three independent experiments ($n = 30–200$ cells per group per experiment). **H** Representative co-localization of nephrin and pMLC2 in three left-most columns and nestin and pMLC2 in right-hand columns. Genotypes and ADR or PBS control treatments are shown at left. In each set, the two individual stains are on either side of the merged image. Fully merged at the rightmost column. Representative of $n = 3$ replicates. Size bar = 10 µm.

during the course of podocyte injury. α3β1 integrin is primarily a laminin receptor[26] and is abundantly expressed by podocyte FPs[27]. The αv integrin subunit is unusual in that it may heterodimerize with several different β subunits. αv integrins bind ECM components such as vitronectin, fibronectin, and several others[28]. Our RNAseq results from isolated murine podocytes (normal or injured) indicated that the most abundantly expressed α and β integrin subunits were α3, αv, β1, and β5[11], and our analysis finds β5 to be abundant in podocytes (Fig. S11), suggesting αvβ5 may be the most prominent αv integrin on normal murine podocytes. αv integrins co-localizing with nephrin are most abundant where podocytes are juxtaposed to the GBM in contact with mesangial cells (Fig. 6Aa), that is also the location where fibronectin is most abundant (Fig. 6Ca)[29]. In contrast, αv integrins were relatively less abundant along capillary loops, particularly those more peripherally located within the glomerulus (Fig. 6Aa). After ADR-induced injury in BALB/c mice, there was an increase in the abundance of αv integrins co-localized with the podocyte protein nephrin, both along capillary loops and where podocytes are juxtaposed to the mesangial matrix (Fig. 6Aa vs. Ab). Quantification of αv integrins showing overlapping staining with synaptopodin (examples shown in Fig. S12) is shown in Fig. 6Ba-c. ADR injury also led to an increase in fibronectin within the glomerulus, that may serve as the ligand for the increased αv integrins (Fig. 6Ca vs. Cb).

The integrin repertoire on podocyte regulates the location of YAP and TAZ

The change in the integrin repertoire of podocytes and in the surrounding extracellular matrix after injury led us to hypothesize that it is a driver of YAP nuclear translocation. Therefore, we used an induced podocyte-specific knockout of *Itga3* in adult mice (Fig. 7A) to create a situation mimicking injury where there is a dramatic change in the adhesive interactions of podocytes with the GBM. Loss of α3β1 integrin resulted in proteinuria by D14 post-induction with tamoxifen (Fig. S13A). αv integrins were more abundant after the loss of α3β1integrin (Fig. S14A–D), as was fibronectin (Fig. 7C), a ligand of αv integrins. Loss of α3β1 integrin also led to decreased activated β1 on capillary loops (Fig. 7A). On the other hand, increased staining for αv (Fig. S14A–C), and β5 (Fig. S14D) integrin subunits was present and extending around capillary loops. Interestingly, the loss of α3β1 integrin did not appear to diminish the amount of total β1 integrin present. Together, these observations suggest that α3β1 integrin is replaced by both αvβ1 and αvβ5 integrins, and that they are responsible for altered mechanosensation at the foot process due to increased fibronectin present after injury. Loss of α3β1 integrin also promoted increased nuclear translocation of YAP (Fig. S15). Our published RNA-seq data indicate that *Fn1* mRNA is present at very low levels in podocytes before or after injury[11]. This suggests that mesangial cells are the primary source of FN, emphasizing the importance of epithelial:stromal (i.e., podocyte:mesangial) interactions in the response to injury.

Activation of integrin αVβ5 results in FAK-dependent nuclear translocation of YAP

To further study the effects of integrin αV activation on YAP localization, we seeded immortalized differentiated podocytes on either laminin or fibronectin-coated plates. Cells plated on laminin spread more than those on fibronectin (Fig. 8A, B). On laminin, α3β1 integrin was localized in linear arrays, and largely overlapped with active β1 (Fig. 8A). In contrast, α3β1 had a more punctate distribution in cells plated on fibronectin, but still largely overlapped with active β1. αv integrins were prominent in cells adhered to fibronectin, but much less so in cells on laminin (Fig. 8B). In either case, αv integrins showed little overlap with activated β1, again consistent with αvβ5 being the major αv integrin on podocytes. Most striking is the very different localization pattern of α3β1 in cells on laminin vs. αv integrins in cells on fibronectin, the latter appearing in a focal adhesion-like pattern at the periphery of the cell, whereas the linear arrays of αβ31 integrin structures were abundant throughout the entire area of the cell. These observations serve to emphasize that distinct integrin-ligand interactions may confer very different behavioral responses, even when present in the same cell type.

YAP was primarily nuclear in cells plated on fibronectin, whereas it was cytoplasmic in cells plated on laminin (Fig. 8C). While there is a variation amongst cells in cultures of differentiated podocytes, small molecule blockers of pan-αv integrins (MK-0249), of Focal Adhesion Kinase (FAK) (PF-573228), or a blocking antibody specific for αvβ5 integrin (ALULA[30]) all reduced nuclear localization of YAP (Fig. 8D is co-stained with pMLC2 to outline cells, quantification in Fig. 8E). These in vitro results support our hypothesis that the increased proportion of αvβ5 to α3β1 integrins and the increased presence of fibronectin after injury are a driver of YAP nuclear translocation.

YAP and integrin changes in human kidney disease

We hypothesized that alteration of YAP/ TAZ expression in differentiated cells results in failure to delay the progression of injury. Consequently, changes in *Yap/Taz* expression in podocytes might alter their ability to generate a proper response to many types of glomerular injuries. In normal human kidney tissue, co-localization of YAP and synaptopodin confirms that YAP is expressed in podocyte nuclei and foot processes (Fig. 9A, control. Fig. 9A with magnified insets is reproduced as Fig. S16). We then examined biopsies of patients who developed glomerular injury of different etiologies. YAP was present, but the co-staining with synaptopodin was mostly lost in glomeruli of biopsy tissue from individuals with FSGS, and entirely in collapsing glomerulopathy and diabetic nephropathy, indicating that YAP was greatly decreased in podocytes but continued to be expressed in mesangial cells in these disease states (Fig. 9A and Fig. S16). The loss of nuclear YAP in podocytes of the collapsing glomerulopathy example is consistent with the phenotype of DKO mice.

Based on our findings that nuclear translocation of YAP was stimulated by αv integrins, we examined the biopsy tissue for glomerular expression of αv integrins. In normal glomeruli, αv expression overlapped with synaptopodin, confirming αv expression in podocytes of human glomeruli (Fig. 9B). In the disease states, there was dramatic over-expression of αv integrins. In the glomeruli from individuals with FSGS, there was partial co-staining with synaptopodin, suggesting it was over-expressed in podocytes and also by cells forming the sclerotic tissue. Co-staining of αv integrins and

https://doi.org/10.1038/s41467-025-58567-y

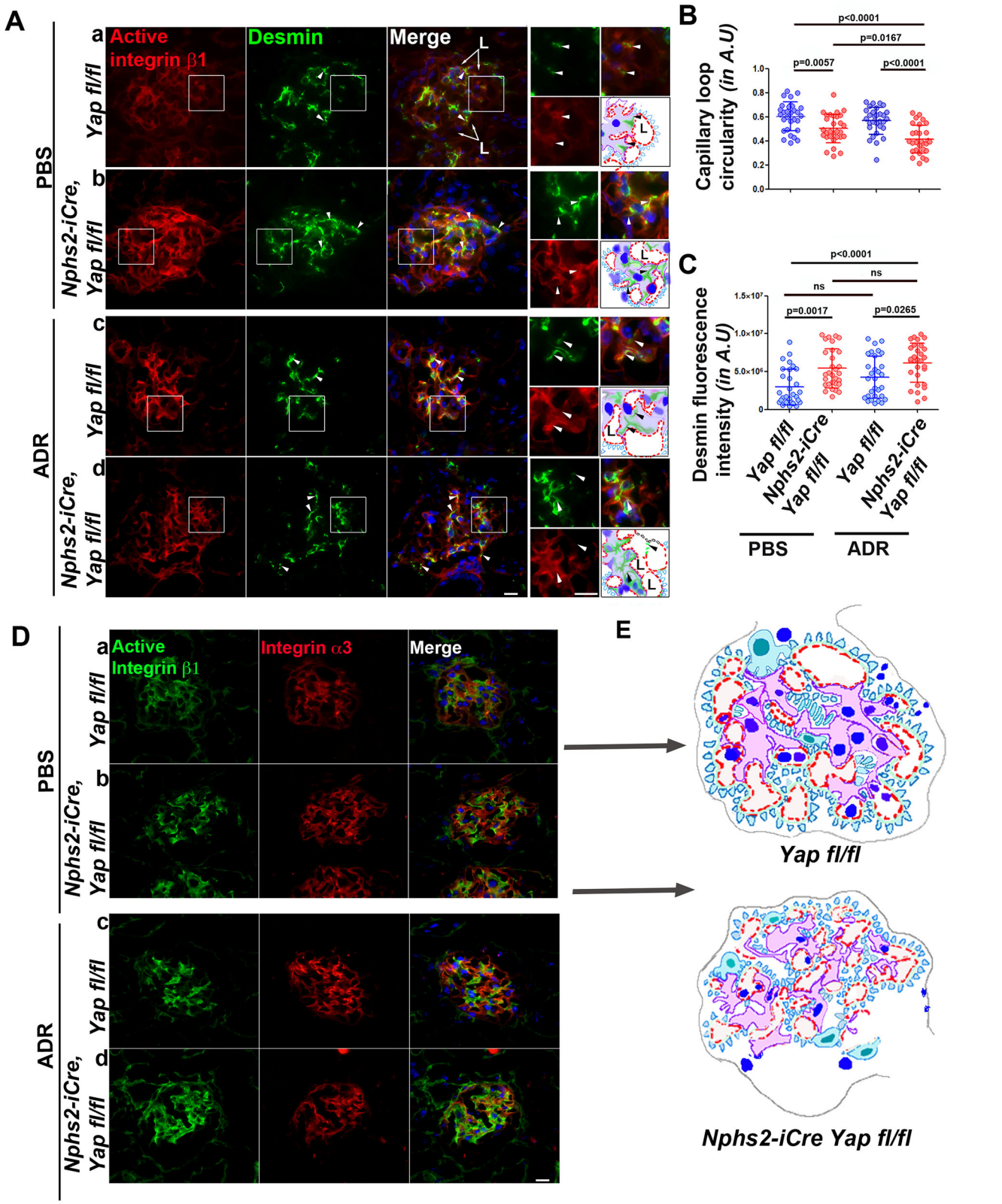

synaptopodin was also prominent in glomeruli representing collapsing glomerulopathy and diabetic nephropathy. Additional examples of glomeruli in these patients show that the increased expression of αv integrin does not correlate with the severity of the lesions, but rather precedes the loss of podocytes (Fig. S17A–C). The overexpression of αv integrins in human biopsy tissue suggests that there is a dramatic change in mechanosensory input into podocytes, that may affect the nuclear localization of YAP and thereby contribute to transcriptional programming that occurs in podocytes during the injury process. This, in many instances, ultimately leads to[12,14,31–35] podocyte loss, collapse of the glomerular vascular bed and glomerulosclerosis.

Fig. 5 | Podocyte-mesangial interaction during podocyte injury depends on YAP. A Co-localization of active β1 integrin (red) and desmin (green). Experimental conditions and genotypes at left of panels and referred to by rows (a–d) in the text. Size bar = 10 µm. The boxes demarcate the insets at the far right. Arrowheads mark the localization of desmin at mesangial pedestals in control, and forming irregular networks in *Yap* mutant and ADR-treated mice. The bottom right panel of each set of insets schematizes the localization of podocytes (FP in blue) and mesangial cells (purple). Capillary loops are outlined in red. **B** Circularity score of capillary loops (see Methods for detailed description). One-way ANOVA with Tukey's multiple comparison test was used, *p* values in figure. $n = 3$ mice per group. **C** Increased desmin fluorescence intensity in *Yap* mutant mice. One-way ANOVA with Tukey's multiple comparison test was used. ns nonsignificant, *p* values in figure. $n = 3$ per group. **D** Co-localization of active β1 integrin (green) and α3β1 integrin (red). Size bar = 10 µm. Representative of $n = 3$ animals per group. **E** Schematic drawings of the glomeruli imaged in rows (Da) and (Db).

Discussion

Previous studies on YAP in podocytes have demonstrated its importance in gene expression, cell survival, assembly of the slit diaphragm and cytoskeleton[12,14,31–35]. Here we have concentrated on the role of YAP/TAZ as a crucial link between cell adhesion and podocyte gene expression. These functions serve as important determinants of capillary loop architecture mediated by interactions between podocytes and mesangial cells. We also demonstrated that YAP is essential in the response to injury. A second focus of our studies has been on how the integrins expressed by podocytes change in response to injury, more prominently increasing the expression of αv integrins. Additionally, the ECM protein fibronectin, a ligand of αv integrins, becomes more abundant after injury (summarized in Fig. 10). Using in vitro experiments, we demonstrated that podocytes behave remarkably differently depending on their underlying matrix. The nuclear translocation of YAP appears to be driven by the interaction of αv integrins with fibronectin. Our previous studies had focused on how the WT1 transcription factor regulates transcriptional reprogramming in the response to injury[11]. The present work extends our understanding of this reprogramming process by demonstrating that YAP/TAZ are transcriptional effectors that, similar to WT1, are essential for maintaining basal podocyte transcription and for the reprogramming that occurs in response to injury. Indeed, we had found predicted TEAD binding motifs commonly adjacent to sites bound by WT1, suggesting that WT1 and the YAP/TAZ-TEAD complex constitute a core set of transcription factors maintaining gene expression.

The regulatory interplay between integrin interaction with the ECM and transcriptional regulation appears to play a crucial role in the podocyte response to injury. Many previous studies have identified a set of transcription factors important to maintain podocyte gene expression, including WT1, FoxC2, Lmx1b, MafB, and TCF21[36–38]. However, our understanding of how transcription factor activity might be affected by changes in the ECM encountered by podocytes is very limited. α3β1 integrin had been identified many years ago as an essential integrin involved in maintaining foot process architecture[9]. More recent studies have demonstrated a role for αv integrins[39,40]. The present study identified αvβ5 as a major integrin in murine podocytes. Our combined observations lead us to propose a model (summarized in Fig. 10) whereby podocyte injury results in increased interaction of αvβ5 integrin with fibronectin and a concomitant decrease in the interaction of α3β1 with laminin. This change in the extracellular environment drives nuclear localization of YAP/TAZ and increased binding of YAP/TAZ to their target genes, such as *Nphs1, Nphs1, Synpo*, and many others, in an effort to repair the GFB. If this effort fails, podocytes detach from the GBM, leading to glomerulosclerosis. This raises the question of whether YAP/TAZ only have a positive role in the response to injury. CTGF is a known transcriptional target of YAP/TAZ[41,42], and it is possible that severe injury leads to the perdurance of YAP binding to target genes such as *Ctgf* that stimulate the expression of genes associated with fibrosis. Thus, an important point of future studies will be to determine whether the set of YAP target genes changes in response to injury, and the underlying mechanisms determining those changes. Moreover, the upstream and downstream relationships between integrin-ECM interactions and YAP-dependent gene expression are likely to be complex, and require further study. One possibility is that a positive feedback loop may be established through which pathological integrin-ECM interactions drive nuclear localization of YAP, and if a repair process is inadequate, continued YAP activity drives a fibrotic instead of a reparative process.

Interactions between stromal and epithelial cells has become increasingly important in understanding many disease processes. In the context of the glomerulus, the interactions of mesangial cells and podocytes is an interesting example of these interactions[5]. Capillary loops within the glomerulus are held in place by a core complex of mesangial cells and their associated matrix, and also by the scaffold formed by podocyte foot processes. That mesangial cells and podocytes constantly exert mechanical forces to maintain capillary loops is suggested by observations that glomeruli appear to have much more abundant activated β1 integrin, revealed by immunostaining, than the surrounding tubules. YAP/TAZ activity within podocytes appears to be essential to maintain those mechanical forces. In the absence of YAP/TAZ, the capillary loop structure and the arrangement of mesangial cells becomes highly disorganized. pMLC is much less abundant in the absence of YAP/TAZ, suggesting that their target genes include those required to maintain the contractile apparatus as a component of the podocyte cytoskeleton. Our observations also bring attention to the concept that within the context of stromal-epithelial interactions, distinct integrin-ECM interactions may occur at different locations on a single highly differentiated cell. Injury may disturb the normal integration of signal inputs derived from these multiple interactions, that is ultimately manifested as pathological cellular behavior.

Methods

Mice

The transgenic *Nphs2-iCre* mouse line was obtained from Dr. Farhard Danesh, Baylor College of Medicine[43]. Double knockout $Wwr1^{fl/fl}$ and $Yap^{fl/fl}$ were purchased from the Jackson Laboratories (Strain #030532). Experiments in single *Yap* knockout animals were carried out from the $Yap^{fl/fl}$ mouse line developed and gifted by Dr. Fernando Camargo (Boston Children's Hospital). $Itga3^{fl/fl}$ mice were previously generated and described[44]. Eight-week-old BALB/C mice were purchased from the Jackson Laboratory *Nphs2-iCre* mice were crossed with mice carrying floxed alleles of $Itga3^{fl/fl}$, $Yap^{fl/fl}$, or $Wwr1^{fl/fl}$. All experiments involving mice were approved by the Institutional Animal Care and Use Committees at Boston Children's Hospital and the Beth Israel Deaconess Medical Center. Mice were housed under standard conditions. Mouse chow: Purina 5008. With the exception of ADR injury experiments, both male and female mice were included in all experiments and yielded equivalent results.

Antibodies and primers

Antibodies are listed in Table S3. Primer sequences in Table S4.

Gene inactivation

Tamoxifen was diluted into 42 °C heated corn oil (Sigma) and injected with a 21G needle (BD) into the peritoneal region of 8-week-old mice. About 200 µl of tamoxifen (150 mg/kg) were injected on two consecutive days.

https://doi.org/10.1038/s41467-025-58567-y

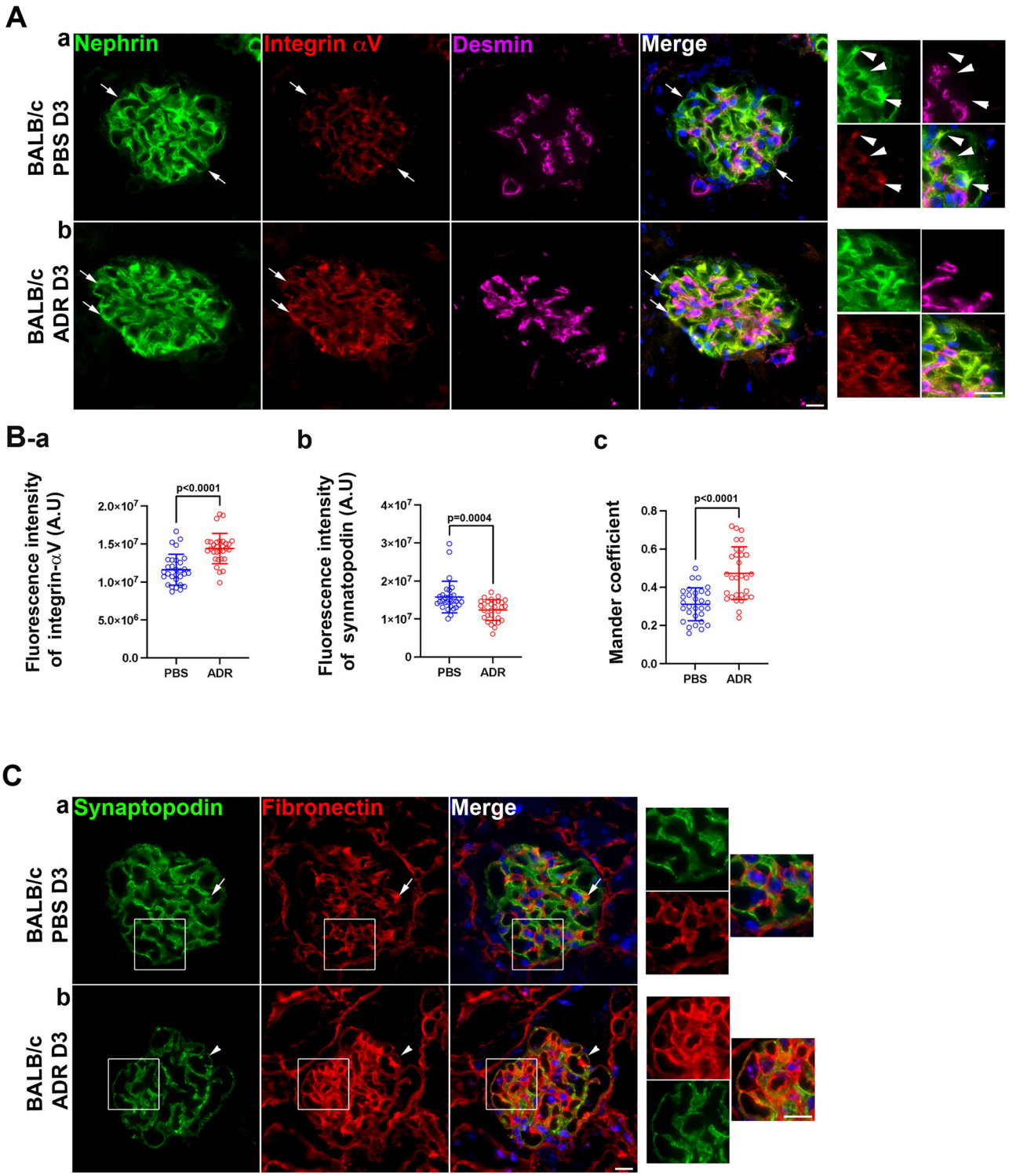

Fig. 6 | Podocyte injury changes the integrin:ECM interactions in the glomerulus. (Aa, Ba, Ca): control glomeruli of BALB/c mice; (Ab, Bb, Cb): Glomeruli from ADR-treated BALB/c mice. **A** Co-localization of nephrin, αv integrins, and desmin. The boxes in all rows demarcate the insets at the far right. Arrows are used to demonstrate the presence of αv integrins on capillary loops, which is greater after injury (Aa vs. Ab). Arrowheads in the inset control panels mark the localization of αv integrins where podocytes oppose mesangial cells. **B** Quantification of integrin αv (**B**a), and Synaptopodin (**B**b) immunofluorescent signals in glomeruli from control and ADR-treated mice plotted as mean values ± SD, Mann–Whitney two-tailed test, *p* values in figure. (Ba). (an example of an image used to quantify staining is shown in Fig. S10). (**B**c) The calculated Mander coefficient relating overlap of αv and synaptopodin (see Methods for details). $n = 3$ per group. **C** Co-localization of fibronectin and synaptopodin. An arrow points to the normal distribution of fibronectin in the control. An arrowhead points out increased fibronectin in a capillary loop of the ADR-treated mouse. Further detailed images are provided in the insets. Representative of $n = 3$ animals per group. Size bars = 10 µm.

https://doi.org/10.1038/s41467-025-58567-y

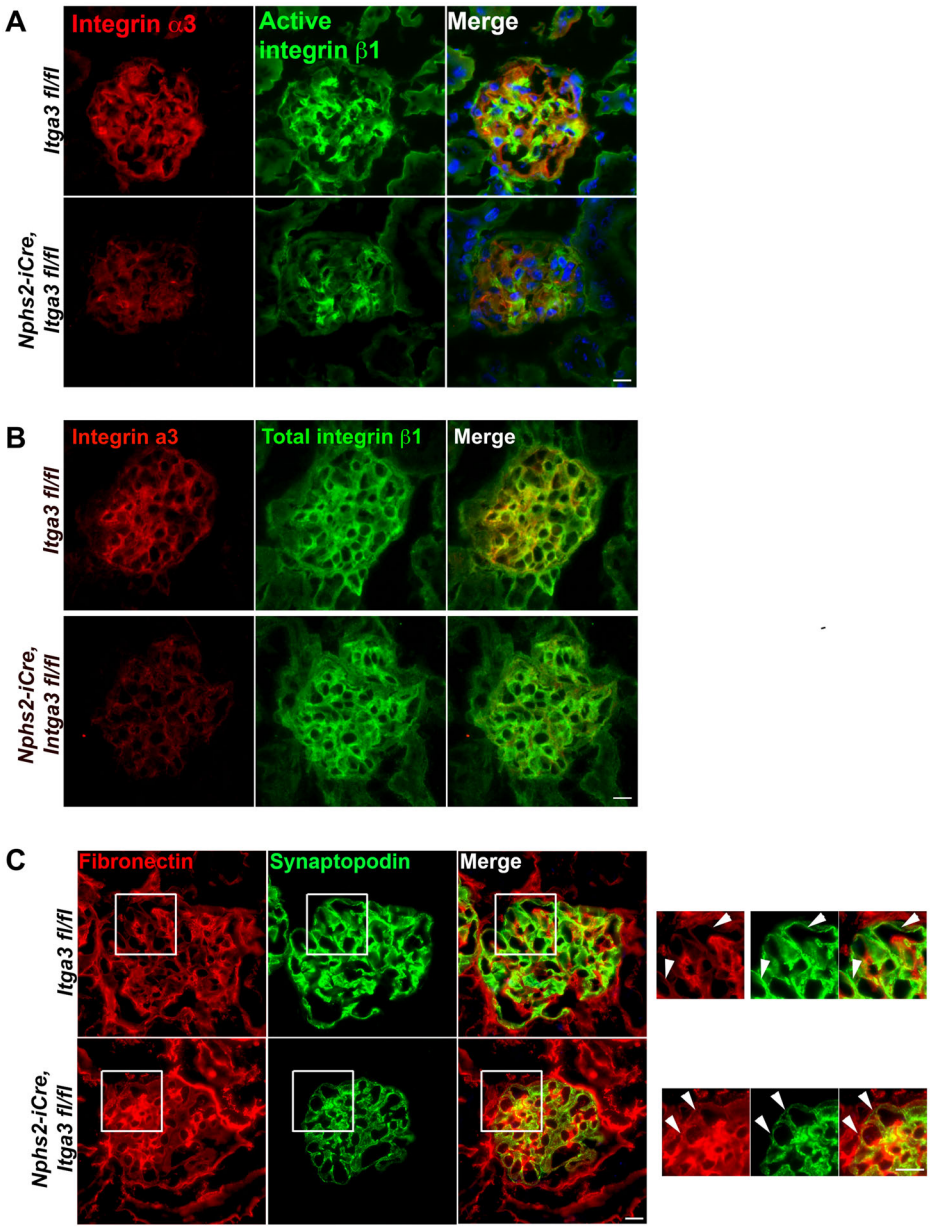

Fig. 7 | Loss of α3β1 integrin in podocytes changes the glomerular ECM. In **A**–**C**, the top row shows control glomeruli from *Itga3*$^{fl/fl}$ mice, and the bottom row shows glomeruli from *Nphs2-iCre, Itga3*$^{fl/fl}$ mice, 14 days post tamoxifen. **A** Co-localization of α3β1 integrin and activated β1 integrin. **B** Co-localization of α3β1 and total β1 integrin. **C** Co-localization of fibronectin and synaptopodin. The boxes in all rows demarcate the insets at the far right representative of $n = 3$ animals per group. Size bar = 10 µm.

Glomerular injury

Male mice 8 weeks old received retro-orbital injections of PBS or Adriamycin (ADR, Cayman Chemicals) under isoflurane anesthesia. Balb/C mice received 10.5 mg/kg ADR. All other mice received 15 mg/kg. For nephrotoxic serum experiments, mice received sheep serum or nephrotoxic serum (NTS) 30 mg/kg. Urine samples were obtained, and kidneys were removed after sacrifice at time points indicated in the text.

Albumin/creatinine ratio (ACR) quantification

About 50 µl of mouse urine was collected for ACR measurement with DCA assays (Siemens). Results were obtained using a Siemens Healthineers DCA Vantage Analyzer (Siemens).

Glomerular isolation

After animal euthanasia, a solution of 5 mL DPBS/50uL tosylactivated dynabeads (Invitrogen) was perfused into each renal arteries using a syringe. Kidneys were then minced, resuspended into digest solution (16 mg pronase (Roche)/500IU DNaseI, 2547U collagenase 1 (Worthington)/8mLHBSS), incubated at 37 °C with constant agitation at 100 rpm for 20 min. During this period, the homogenate was resuspended with a pipet boy every 5 min. The homogenate is then sieved through a 100-um cell strainer, followed by an HBSS wash. Flow through was collected and filtered again with a new 100 uM cell strainer, followed by an HBSS rinse. The eluate was spun for 5 min 4 °C at 1500 rpm. The supernatant was discarded and the pellet was washed with HBSS. Four additional washes-centrifugation series were processed to efficaciously remove the tubules. After the completion of the wash-centrifugation steps, the pellet was resuspended into 4 mL of HBSS and put into a magnet concentrator, then washed three times. The glomeruli-enriched fractions are located with the magnetic beads and can be treated with lysis buffer. For protein extraction, see bellow the western blot section.

https://doi.org/10.1038/s41467-025-58567-y

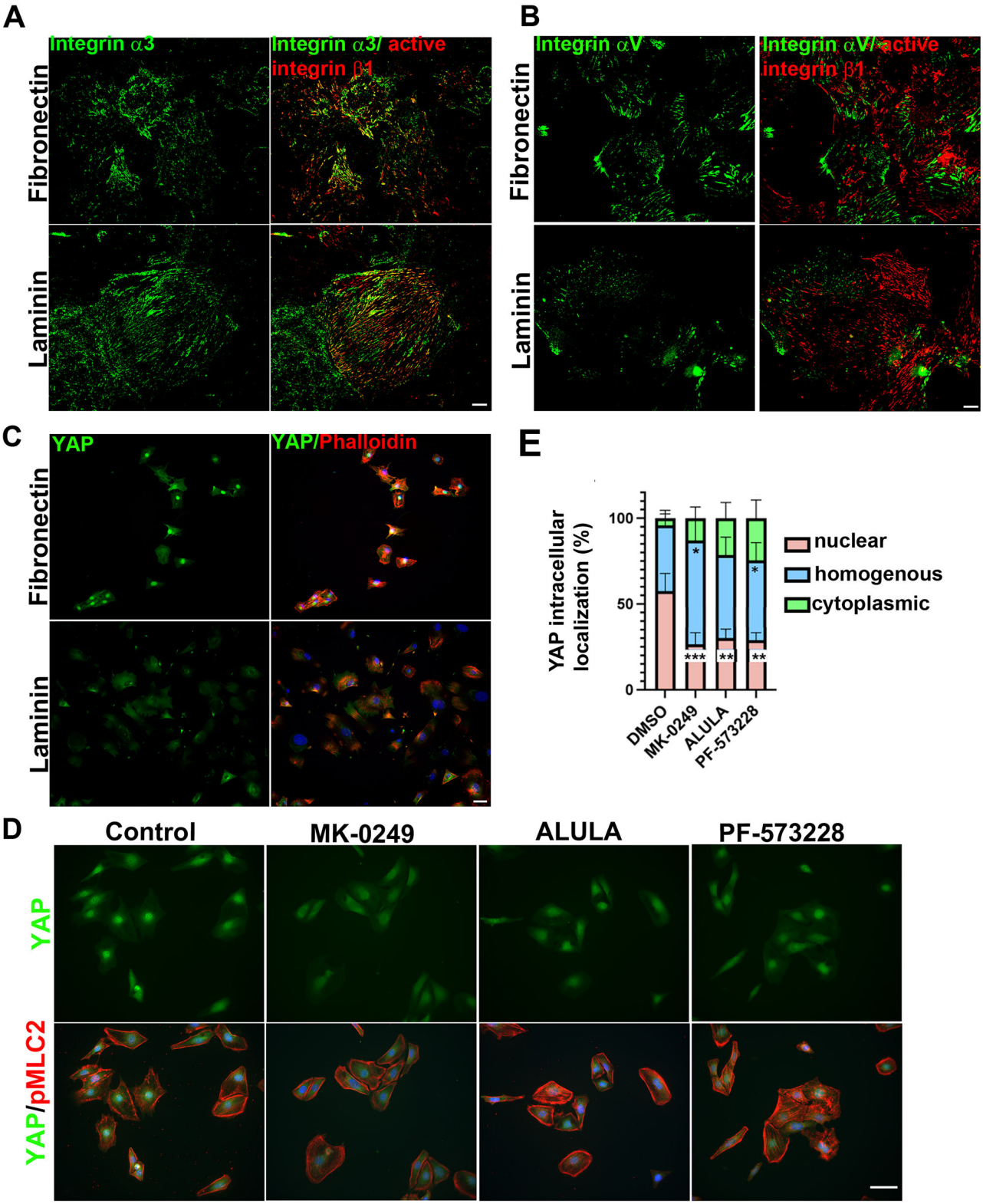

Fig. 8 | αvβ5 integrin drives nuclear localization of YAP. A Immortalized podocytes are plated on fibronectin (top panels) or laminin (bottom panels). α3β1 integrin-green, activated β1 integrin-red. **B** same conditions as (**A**), αv integrins-green, activated β1 integrin-red. Size bar = 20 µm. **C** YAP (green) localization, co-stained with phalloidin (red). same conditions as (**A**). Size bar = 50 µm. **D** YAP localization (top row) and co-localization with pMLC2 (red). Treatment at the top of each panel. MK-0249- pan αv integrin inhibitor; ALULA- monoclonal antibody specific blocker of αvβ5 integrin; PF-573228-inhibitor of FAK. Size bar = 50 µm. **E** Quantification of YAP localization shown in (**D**), plotted as mean values ± SD, representative of three independent experiments. Two-way ANOVA with Sidak's multiple comparison test was used. Nuclear (pink bars) $^{***}p = 0.0005$ (MK-0249 vs. control), $^{*}p = 0.0018$(ALULA vs control), $^{**}p = 0.0011$ (PF-573228 vs. control); Homogeneous (blue bars) $^{*}p = 0.014$ (MK-0249 vs. control), $^{*}p = 0.0218$ (PF-573228 vs. control). $n = 3$ independent experiments ($n = 50$ cells per group per experiment).

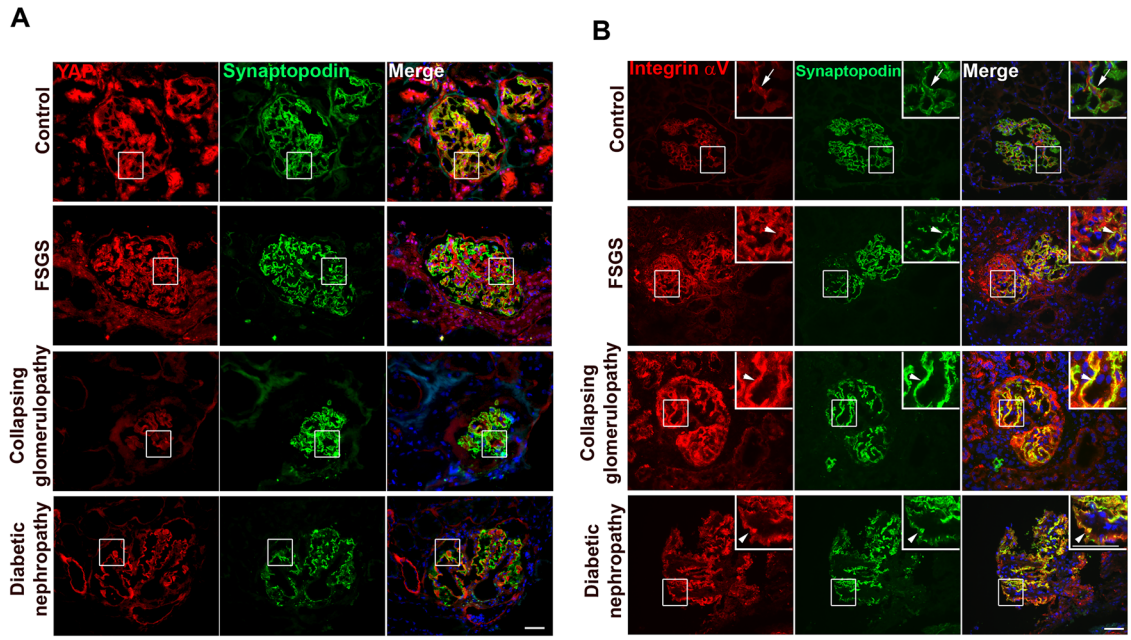

Fig. 9 | YAP and αv integrins in human glomerular pathology. The pathological diagnosis is at the left of each row. **A** Co-localization of YAP and synaptopodin. In the normal kidney, YAP overlaps with DAPI. In the FSGS example, few podocyte nuclei contain YAP. In the collapsing glomerulopathy example, YAP appears not to be present in podocyte nuclei, marked by arrowheads. In the diabetic nephropathy example, YAP similarly appears not to be present in most podocyte nuclei. **A** is reproduced with magnified insets in Fig. S16. **B** Co-localization of αv integrins and synaptopodin. The arrowheads in insets mark examples of adjacent localization of αv integrins and synaptopodin. Representative of $n = 3$ biopsy specimens. Size bar = 50 µm.

Cell culture

All in vitro experiments utilized a previously published line of immortalized differentiated mouse podocytes[45]. This line was derived using the immortomouse according to published protocols[46] (Charles River Laboratories, Wilmington, MA, USA). To induce differentiation, cells were maintained for 14 days at 37 °C without IFN-γ[46]. For inhibitor and antibody treatments, podocytes were incubated with 10 ug/ml of integrin αVβ5/ALULA monoclonal antibody[30], or with 0.5 nM of MK 0429 (Medchem express), for 3 h or with 10 uM of PF-573228 (Medchem express) for 2 h.

Gene knockdown in vitro

siRNAs were purchased from Thermo Fisher. 5′-CCAAUAGUUC CGAUCCCUUUCUUA-3′ and 5′-UUAAGAAAGGGAUCGGAACUAUUG G-3′ were respectively referred as "si1 *Yap*" and "si2 *Yap*" in the manuscript. About 10 nM of siRNA were transfected with Lipofectamine RNAi max (Thermo Fisher) according to the manufacturer's recommendations for 48 h. After knockdown, podocytes were detached with Trypsin (Gibco). For cell spreading assays, 30,000 cells were seeded into a 24-well plate containing coverslips coated with 50 ug/mL of rat-tail collagen type 1 (Corning). For other types of matrices, 10,000 cells were allowed to spread for 48 h on coverslips coated with either 5 ug/ml of laminin 521 (Biolamina) or with 50 ug/mL of fibronectin (Thermo Fisher).

Western blot

Whole-cell lysates from cultured podocytes or from isolated glomeruli were incubated with RIPA buffer (300 mM NaCl, 50 mM Tris-HCl (pH 7.4), 5 mM EDTA, 0.1% SDS, 1% Igepal, 0.5% sodium deoxycholate), supplemented with anti-phosphatase and protease inhibitor cocktail (Roche). Protein quantification was conducted using the BCA protein assay kit (Thermo Scientific). Samples were loaded onto SDS–polyacrylamide gel. A standard western blot was conducted with the indicated antibodies in Supplementary Table 1. Quantification of western blots as in ref. 11.

Immunofluorescence analysis

About 2-µm-thick sections from kidneys embedded in OCT were fixed with 2% PFA/PBS, (Exceptions: fibronectin staining used 0.5% PFA/PBS; staining nuclear proteins used 4% PFA/PBS followed by 30% of sucrose/PBS for 15 min and then permeabilization with 0.1% Triton X-100 for 5 min). Slides were then treated with a blocking buffer (2% BSA, 5% normal donkey in PBS) at room temperature. Primary antibodies were diluted into a blocking buffer and applied to slides for 16 h at 4 °C. After PBS washes, samples were treated with appropriate Alexa fluor coupled-secondary antibodies (Invitrogen). Finally, tissue sections were washed with PBS before mounting with Prolong Gold supplemented with DAPI (Thermo Fisher). Samples were imaged using a Nikon Eclipse Ni microscope.

For staining of immortalized podocytes, cells were fixed with 4% PFA/PBS and conducted as described with tissue sections with the exception of integrin α3 and αV stainings (see below). WT1 and YAP detection included permeabilization with 0.1% Triton X-100 for 5 min. For detection of integrin α3β1 and αV, cells were rinsed with PBS supplemented with calcium chloride and magnesium chloride (PBS ++, Corning), before chemical cross-linking with 0.4 mM of BS3 (Thermo Fisher) at room temperature for 10 min[47]. About 10 mM Tris-HCL pH 7.5 was used to quench the aldehyde groups. Cells were then rinsed with PBS ++ and incubated for 20 min at room temperature with 0.5% NP40/PBS supplemented with anti-protease. Immunostaining proceeded with the regular tissue protocol at the fixation step.

Quantification of immunofluorescence staining

Quantification of paxillin staining in Supplementary Fig. 5C–E, was performed using the FIJI program with the "Analyze particle" tool as previously described[48]. 15 pictures/experiment ($n = 3$) were taken at 40X magnification. Background was substracted with FIJI, then threshold command was applied. The analyze particles tool was used to automatically determine the number of focal adhesions and their sizes. The quantification of the fluorescence intensity of YAP in podocyte nuclei in Fig. 3A, B and S4 was performed on kidney sections

https://doi.org/10.1038/s41467-025-58567-y

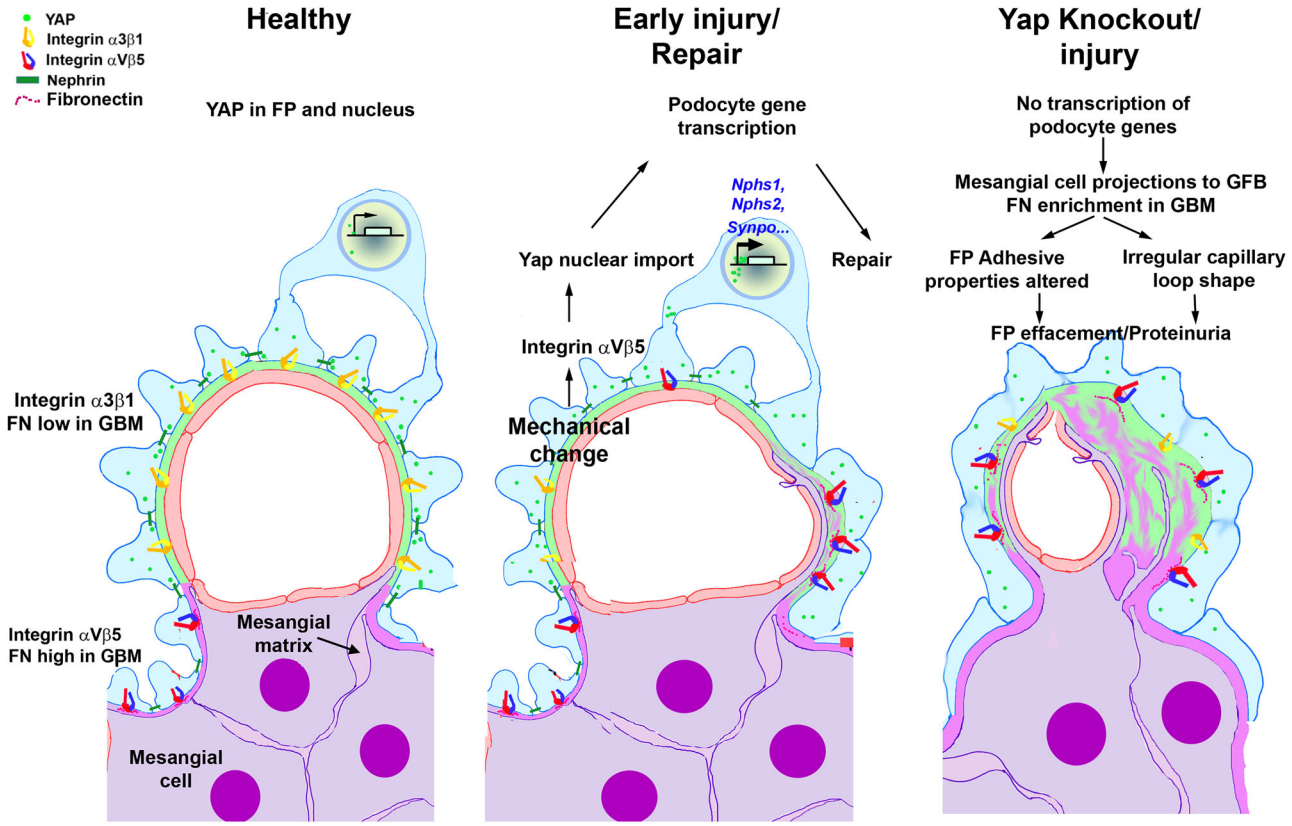

Fig. 10 | Model for integrin and YAP/TAZ function in podocyte injury. Left: A healthy capillary loop, with α3β1 integrin primarily where foot processes adhere to the GBM. αvβ5 integrin is primarily at the mesangial pedestal. Middle: A capillary loop at an early injury/repair stage. αvβ5 integrin and fibronectin are present around the entire capillary loop, and YAP/TAZ translocates to the nucleus to increase the expression of proteins required to maintain the GFB. This allows foot process repair. Right: In situations of irreversible injury, including injury of *Yap* mutant mice, there is foot process effacement, increased abundance of αvβ5 integrin and fibronectin, and eventual sclerosis.

co-stained with antibodies against YAP and p57 (see table of antibodies). 15 pictures/experiment ($n = 3$) were taken at 63X magnification. The mean intensity of the YAP nuclear signal is measured in cells that are positive for p57 staining. The background signal was subtracted and the intensity of the signal was normalized to the area.

Quantification of circularity scores in Fig. 5: Capillary circularity was determined using the shape descriptor function in ImageJ. Pictures from nephrin staining at 100X magnification were used to delineate all capillary loops within a glomerulus before circularity analysis. The average value from all capillary loops is reported. Ten glomeruli per animal ($n = 3$–4 animals per group) were analyzed for capillary morphology. Two-way ANOVA with Dunnett's multiple comparison test was used.

Calculation of Mander coefficient in Fig. 6: Co-localization analysis was performed in ImageJ with JACoP plugin as described previously[49]. Briefly, for each image taken at the magnification of 100X, the glomerulus is defined and selected via synaptopodin staining. The same threshold was applied to every image in order to reduce the background signal. Mander's coefficients were calculated for the synaptopodin (green channel) and integrin αV (red channel). Mander's coefficient for synaptopodin, is used as an indicator of the proportion of green pixels (synaptopodin) that overlap with red pixels (integrin αV) above background, and is represented in the graph. Ten glomeruli per animal ($n = 3$–4 per group) were quantified for co-localization analysis. An unpaired *t*-test using GraphPad Prism generated the statistical analysis.

For quantification of synaptopodin and integrin αV fluorescence intensity in Fig. S12, background subtraction and threshold application were performed as mentioned above, before using the CTCF (corrected total cell fluorescence) method to perform semi quantification of fluorescence analysis. Ten glomerular images taken at 100X magnification per animal ($n = 3$–4 animals per group) were analyzed for capillary morphology. As described above, an unpaired *t*-test was used for statistical analysis.

RNA extraction, cDNA, and RT-qPCR analysis

Extraction of total RNA from cultured mouse podocytes and glomeruli was performed using TRIzol Reagent (Invitrogen). Complementary DNAs were synthesized using a Superscript III reverse transcriptase kit (Invitrogen) according to the manufacturer's protocol. RT-qPCR was running using this thermal cycling program: 95 °C for 5 min, 40 cycles of 5 s at 95 °C, 5 s at 60 °C, and 10 s at 72 °C, followed by a final 5-min extension at 72 °C. mRNA expressions of the genes of interest were normalized to *Gapdh* mRNA expression using the $\Delta\Delta C_t$ method. The list of primers used are listed in the Supplementary Table 2.

ChIP-qPCR

Chromatin immunoprecipitation (ChIP) assays were conducted in 8-week-old BALB/cJmice, or 10 days after tamoxifen induction in *Nphs2-iCre Wwr1*$^{fl/fl}$,*Yap* $^{fl/fl}$ mice. Glomerular extracts from two mice were pooled to isolate the chromatin required for the ChIP as previously described[11]. Immunoprecipitation was performed overnight at 4 °C with anti-YAP (Abcam) or with an isotype control anti-IgG rabbit (Santa Cruz). The following day, Dynabeads (Invitrogen) were incubated for 2 h 30 before washes. Chromatin was recovered by phenol-chloroform extraction and ethanol precipitation. RT-qPCR

analyses were performed on immunoprecipitated DNA using specific primers described in Supplementary Table 1. Fold enrichment of ChIP versus immunoglobulin G (IgG) control was calculated as $2((C_t(\text{IgG}) - C_t(\text{input})) - (C_t(\text{ChIP}) - C_t(\text{input})))$.

Statistical analysis

Statistical analysis were conducted with GraphPad Prism 9 software (San Diego, CA, United States). Results were compared using one-way or two-way ANOVA tests for multiple group comparisons. The Mann–Whitney *U*-test was employed for paired groups. The specific tests used in the statistical analyses and their *p* values associated with the comparison are indicated in each figure legend.

Reporting summary

Further information on research design is available in the Nature Portfolio Reporting Summary linked to this article.

Data availability

Full quantitative data supporting figures and full western blots are found in the Source file. For figures that contain representative histological or immunofluorescent images, additional images will be provided upon request. Source data are provided with this paper.

References

1. Andrews, C., McLean, M. H. & Durum, S. K. Cytokine tuning of intestinal epithelial function. *Front. Immunol.* **9**, 1270 (2018).
2. Zhang, Y., Crawford, H. C. & Pasca di Magliano, M. Epithelial-stromal interactions in pancreatic cancer. *Annu. Rev. Physiol.* **81**, 211–233 (2019).
3. Totaro, A., Castellan, M., Di Biagio, D. & Piccolo, S. Crosstalk between YAP/TAZ and Notch signaling. *Trends Cell Biol.* **28**, 560–573 (2018).
4. Malik, R., Lelkes, P. I. & Cukierman, E. Biomechanical and biochemical remodeling of stromal extracellular matrix in cancer. *Trends Biotechnol.* **33**, 230–236 (2015).
5. Avraham, S., Korin, B., Chung, J. J., Oxburgh, L. & Shaw, A. S. The mesangial cell - the glomerular stromal cell. *Nat. Rev. Nephrol.* **17**, 855–864 (2021).
6. Kopp, J. B. et al. Podocytopathies. *Nat. Rev. Dis. Prim.* **6**, 68 (2020).
7. Johansen, K. L. et al. US renal data system 2021 annual data report: epidemiology of kidney disease in the United States. *Am. J. Kidney Dis.* **79**, A8–A12 (2022).
8. Schordan, S., Schordan, E., Endlich, K. & Endlich, N. AlphaV-integrins mediate the mechanoprotective action of osteopontin in podocytes. *Am. J. Physiol. Ren. Physiol.* **300**, F119–F132 (2011).
9. Kreidberg, J. A. et al. Alpha 3 beta 1 integrin has a crucial role in kidney and lung organogenesis. *Development* **122**, 3537–3547 (1996).
10. van Soldt, B. J. & Cardoso, W. V. Hippo-Yap/Taz signaling: complex network interactions and impact in epithelial cell behavior. *Wiley Interdiscip. Rev. Dev. Biol.* **9**, e371 (2020).
11. Ettou, S. et al. Epigenetic transcriptional reprogramming by WT1 mediates a repair response during podocyte injury. *Sci. Adv.* **6**, eabb5460 (2020).
12. Chung, J. J. et al. Single-cell transcriptome profiling of the kidney glomerulus identifies key cell types and reactions to injury. *J. Am. Soc. Nephrol.* **31**, 2341–2354 (2020).
13. Schwartzman, M. et al. Podocyte-specific deletion of Yes-associated protein causes FSGS and progressive renal failure. *J. Am. Soc. Nephrol.* **27**, 216–226 (2016).
14. Chen, J., Wang, X., He, Q. & Harris, R. C. TAZ is important for maintenance of the integrity of podocytes. *Am. J. Physiol. Ren. Physiol.* **322**, F419–F428 (2022).
15. Wang, Y., Wang, Y. P., Tay, Y. C. & Harris, D. C. Progressive adriamycin nephropathy in mice: sequence of histologic and immunohistochemical events. *Kidney Int.* **58**, 1797–1804 (2000).
16. Leardkamolkarn, V., Salant, D. J. & Abrahamson, D. R. Loss and rearrangement of glomerular basement membrane laminin during acute nephrotoxic nephritis in the rat. *Am. J. Pathol.* **137**, 187–198 (1990).
17. Pisarek-Horowitz, A. et al. Loss of roundabout guidance receptor 2 (Robo2) in podocytes protects adult mice from glomerular injury by maintaining podocyte foot process structure. *Am. J. Pathol.* **190**, 799–816 (2020).
18. Verma, R. et al. Shp2 associates with and enhances nephrin tyrosine phosphorylation and is necessary for foot process spreading in mouse models of podocyte injury. *Mol. Cell Biol.* **36**, 596–614 (2016).
19. O'Meara, Y. M. et al. Nephrotoxic antiserum identifies a beta 1-integrin on rat glomerular epithelial cells. *Am. J. Physiol.* **262**, F1083–F1091 (1992).
20. Kuhn, S. & Geyer, M. Formins as effector proteins of Rho GTPases. *Small GTPases* **5**, e29513 (2014).
21. Gauthier, N. C., Masters, T. A. & Sheetz, M. P. Mechanical feedback between membrane tension and dynamics. *Trends Cell Biol.* **22**, 527–535 (2012).
22. Zimmerman, S. E. et al. Nephronectin regulates mesangial cell adhesion and behavior in glomeruli. *J. Am. Soc. Nephrol.* **29**, 1128–1140 (2018).
23. Elbediwy, A. & Thompson, B. J. Evolution of mechanotransduction via YAP/TAZ in animal epithelia. *Curr. Opin. Cell Biol.* **51**, 117–123 (2018).
24. Elbediwy, A. et al. Integrin signalling regulates YAP and TAZ to control skin homeostasis. *Development* **143**, 1674–1687 (2016).
25. Elbediwy, A., Vincent-Mistiaen, Z. I. & Thompson, B. J. YAP and TAZ in epithelial stem cells: a sensor for cell polarity, mechanical forces and tissue damage. *Bioessays* **38**, 644–653 (2016).
26. Gehlsen, K. R., Dickerson, K., Argraves, W. S., Engvall, E. & Ruoslahti, E. Subunit structure of a laminin-binding integrin and localization of its binding site on laminin. *J. Biol. Chem.* **264**, 19034–19038 (1989).
27. Korhonen, M., Ylanne, J., Laitinen, L. & Virtanen, I. The alpha 1-alpha 6 subunits of integrins are characteristically expressed in distinct segments of developing and adult human nephron. *J. Cell Biol.* **111**, 1245–1254 (1990).
28. Vega, M. E. & Schwarzbauer, J. E. Collaboration of fibronectin matrix with other extracellular signals in morphogenesis and differentiation. *Curr. Opin. Cell Biol.* **42**, 1–6 (2016).
29. Courtoy, P. J., Kanwar, Y. S., Hynes, R. O. & Farquhar, M. G. Fibronectin localization in the rat glomerulus. *J. Cell Biol.* **87**, 691–696 (1980).
30. Su, G. et al. Integrin alphavbeta5 regulates lung vascular permeability and pulmonary endothelial barrier function. *Am. J. Respir. Cell Mol. Biol.* **36**, 377–386 (2007).
31. Bonse, J. et al. Nuclear YAP localization as a key regulator of podocyte function. *Cell Death Dis.* **9**, 850 (2018).
32. Chen, J. et al. Inhibition of transcriptional coactivator YAP Impairs the expression and function of transcription factor WT1 in diabetic podocyte injury. *Kidney Int.* **105**, 1200–1211 (2024).
33. Gilhaus, K. et al. Activation of Hippo pathway damages slit diaphragm by deprivation of ajuba proteins. *J. Am. Soc. Nephrol.* **34**, 1039–1055 (2023).
34. Meliambro, K. et al. The Hippo pathway regulator KIBRA promotes podocyte injury by inhibiting YAP signaling and disrupting actin cytoskeletal dynamics. *J. Biol. Chem.* **292**, 21137–21148 (2017).
35. Rinschen, M. M. et al. YAP-mediated mechanotransduction determines the podocyte's response to damage. *Sci. Signal* **10**, eaaf8165 (2017).

36. Quaggin, S. E. & Kreidberg, J. A. Development of the renal glomerulus: good neighbors and good fences. *Development* **135**, 609–620 (2008).
37. Rane, M. J., Zhao, Y. & Cai, L. Krupsilonppel-like factors (KLFs) in renal physiology and disease. *EBioMedicine* **40**, 743–750 (2019).
38. Schell, C., Wanner, N. & Huber, T. B. Glomerular development-shaping the multi-cellular filtration unit. *Semin. Cell Dev. Biol.* **36**, 39–49 (2014).
39. Madhusudhan, T. et al. Podocyte integrin-beta 3 and activated protein C coordinately restrict RhoA signaling and ameliorate diabetic nephropathy. *J. Am. Soc. Nephrol.* **31**, 1762–1780 (2020).
40. Hayek, S. S. et al. A tripartite complex of suPAR, APOL1 risk variants and alphavbeta3 integrin on podocytes mediates chronic kidney disease. *Nat. Med.* **23**, 945–953 (2017).
41. Wang, Q. et al. TAZ promotes epithelial to mesenchymal transition via the upregulation of connective tissue growth factor expression in neuroblastoma cells. *Mol. Med. Rep.* **11**, 982–988 (2015).
42. Fujii, M. et al. Convergent signaling in the regulation of connective tissue growth factor in malignant mesothelioma: TGFbeta signaling and defects in the Hippo signaling cascade. *Cell Cycle* **11**, 3373–3379 (2012).
43. Wang, J. et al. Tamoxifen-inducible podocyte-specific iCre recombinase transgenic mouse provides a simple approach for modulation of podocytes in vivo. *Genesis* **48**, 446–451 (2010).
44. Liu, Y. et al. Coordinate integrin and c-Met signaling regulate Wnt gene expression during epithelial morphogenesis. *Development* **136**, 843–853 (2009).
45. Schumacher, V. A. et al. WT1-dependent sulfatase expression maintains the normal glomerular filtration barrier. *J. Am. Soc. Nephrol.* **22**, 1286–1296 (2011).
46. Mundel, P. et al. Rearrangements of the cytoskeleton and cell contacts induce process formation during differentiation of conditionally immortalized mouse podocyte cell lines. *Exp. Cell Res.* **236**, 248–258 (1997).
47. DiPersio, C. M., Shah, S. & Hynes, R. O. alpha 3A beta 1 integrin localizes to focal contacts in response to diverse extracellular matrix proteins. *J. Cell Sci.* **108**, 2321–2336 (1995).
48. Horzum, U., Ozdil, B. & Pesen-Okvur, D. Step-by-step quantitative analysis of focal adhesions. *MethodsX* **1**, 56–59 (2014).
49. Remuzzi, A. et al. Role of ultrastructural determinants of glomerular permeability in ultrafiltration function loss. *JCI Insight* **5**, e137249 (2020).

Acknowledgements

The authors are grateful to acknowledge Drs. Dean Sheppard (UCSF) for the ALULA monoclonal antibody and David Salant (Boston University) for NTS; Terri Woo and Colleen Ford (Brigham and Women's Hospital) for electron micrograph preparations, and Xuehui Yang for assistance with histological preparations. Support: NIH R01 DK109972 and DOD PR211099 to J.A.K.

Author contributions

E.H.-C., V.D., S.E., S.K., and V.A.S. performed experiments. K.K. and A.W. provided human histological material. A.A. derived and supplied the ALULA antibody. M.E.T. provided experimental support and assisted with mouse husbandry. A.W. performed pathological analyses. Statistical analyses were performed by E.H.-C. and V.A.S. Experiments were designed and analyzed by E.H.-C., V.A.S., and J.A.K.

Competing interests

The authors declare no competing interests.

Additional information

Supplementary information The online version contains supplementary material available at https://doi.org/10.1038/s41467-025-58567-y.

Correspondence and requests for materials should be addressed to Valerie A. Schumacher or Jordan A. Kreidberg.

Peer review information *Nature Communications* thanks the anonymous reviewer(s) for their contribution to the peer review of this work. A peer review file is available.